International Journal of Sciences: Basic and Applied Research (IJSBAR)

ISSN 2307-4531
(Print & Online)

https://gssrr.org/index.php/JournalOfBasicAndApplied/index

Real-Time Adaptive Background-Oriented Schlieren Imaging Algorithm with Spatiotemporal Variability Using Computer Vision and Particle Image Velocimetry

Dhruv Hegde[a*],Tejash Gupta[b],Vikram Haran[c]

[a]*Salem High School, Canton, MI*
[b]*Fulton Science Academy Private School, Alpharetta, GA*
[c]*Academy of Aerospace and Engineering, Windsor, CT*
[a]*Email: dhegderesearch@gmail.com*
[b]*Email: tejash.gupta045@gmail.com*
[c]*Email: Vikram.Haran@gmail.com*

Abstract

This study presents an advanced Background Oriented Schlieren (BOS) computational system designed for high-efficiency, high-resolution fluid flow visualization on mobile platforms. The system integrates wavelet transformations for multi-scale edge detection, Kalman filtering for noise reduction, and adaptive contrast enhancement using CLAHE. The results demonstrate improvements of 30.6% in edge detection sensitivity, 12.5% in resolution enhancement, and 11% in noise reduction, compared to the standard OpenCV and OpenPIV control algorithm. These metrics were calculated through rigorous image processing techniques, including the Laplacian of the image and gradient magnitude for edge detection, full-width at half-maximum (FWHM) for resolution, signal-to-noise resolution (SNR) for noise, and the Jaccard index for flow visualization accuracy.

Received: 8/10/2024
Accepted: 10/1/2024
Published: 10/12/2024

----

* Corresponding author.

The system's ability to deliver accurate and detailed flow visualizations in real time makes it particularly suited for mobile applications, where computational resources are limited. The combination of wavelet analysis, predictive filtering, and adaptive contrast enhancement offers a robust solution for capturing subtle flow patterns, making this approach a significant advancement in BOS technology, with potential application in experimental fluid dynamics, aerodynamic testing, and environmental monitoring.

Keywords: Algorithms; Spatiotemporal Variability; Computer Vision; Particle Image Velocimetry**.**

1. Introduction

1.1 Background Oriented Schlieren (BOS) Imaging

Background Oriented Schlieren (BOS) imaging is an optical technique employed to visualize and quantify refractive index variations induced by density gradients within transparent media such as air [1]. BOS imaging is founded upon the principles of traditional Schlieren photography. Still, it diverges from the foundational knife-edge principle to relying more on a textured plot background, enhancing adaptability to diverse experimental conditions and ameliorating imaging efficiency [2]. The core mechanism with BOS imaging involves capturing the apparent displacement of background features as light traverses regions of varying refractive index caused by artificial gradients within the air.

The displacement of these background features, induced by refractive index gradients as mentioned previously, is measured using Digital Image Correlation (DIC) algorithms, which compare the position of each background point to the undisturbed reference image with its shifted position in the distributed image [3]. This process quantifies the local refractive index gradient with high precision. One constraint within this imaging method is BOS's varying sensitivity to minute density variations, which depends on the resolution of the cameras and recording instruments used. Compared to traditional Schlieren methods, more precise calibration and greater resilience to vibrations are needed in BOS; more accurate calibration of recording materials and greater resilience to vibrations are required within this contemporary imaging process compared to others, including traditional Schlieren itself [4].

Air density gradients, the cause behind the observed distortions, manifest due to temperature, pressure, and composition variations within a given flow field. Flow fields are characterized by complex interactions of the aforementioned factors about the Navier-Stokes equations, which encapsulate the conservation laws of mass, momentum, and energy within the aerodynamic airflow. Incompressible flow fields are primarily governed by velocity distributions, while compressible flow fields, a major focus for this particular study due to prominence in unregulated and uncontrolled environments such as the outside world, also account for significant variations in pressure and temperature. The ideal gas law describes the emergence of air density gradients from temperature gradients, Bernoulli's principle, and compositional variation equations. Temperature-induced density gradients are common in thermal conversion and combustion processes, where heat transfer results in buoyancy-driven flows. Pressure-induced density gradients, another regular underlying factor for compressible flow, are prominent in situations where boundary layers are formed, such as higher-speed air with greater Reynold's number — the ratio of inertial forces to viscous forces within a confined fluid field — or environments where separative structures are introduced. Simulated testing of these conditions through virtual models can be performed through the use of refined Computational Fluid Dynamics (CFD) models, but their accuracy in testing scenarios is limited, and high-speed BOS imaging enables the capture of transient flow phenomena with temporal resolution sufficient to exceed the accuracy and reliability of CFD models [5].

To address the previously mentioned constraint, our project proposes the integration of spatiotemporal variability techniques, which involves the analysis of changes in spatial patterns over time, into BOS imaging through advanced numeric algorithms in Python that result in a more refined visual output. Addressing the sensitivity constraints of BOS through the integration of such techniques can enhance the precision of refractive index gradient measurements, enabling more accurate visualization of complex aerodynamic and fluid dynamic phenomena and significantly improving the analysis of thermal convection processes and high-speed natural flows.

In recent years, advancements in BOS imaging have increasingly leveraged open-source platforms such as OpenCV and OpenPIV to create more accessible and customizable BOS frameworks. These tools offer extensive libraries for image processing, which facilitate the development of real-time flow visualization systems with a high degree of flexibility. One notable project is the IIT-developed Pocket Schlieren, which uses a mobile phone to capture schlieren-like images with OpenCV processing. While this innovation brings BOS imaging to a more portable format, it has significant drawbacks. The resolution and accuracy of Pocket Schlieren are highly dependent on the mobile camera's quality, limiting its ability to detect fine refractive index gradients or turbulent flow in high-speed or large-scale environments. Moreover, the absence of advanced calibration techniques and limited control over lighting conditions mean that this setup struggles under varying or uncontrolled flow conditions, such as those encountered in outdoor testing or supersonic applications. The simplicity of its setup is both an advantage for portability and a limitation for precision, as it cannot match the sensitivity and robustness of traditional high-resolution BOS systems or our more refined system that incorporates dynamic background subtraction and wavelet transformations for improved accuracy.

1.2 Spatiotemporal Variability Techniques

Spatiotemporal variability refers to changes in visual data points across both spatial and temporal dimensions, capturing how patterns evolve and space. In the context of video processing, spatiotemporal variability techniques analyze sequences of images to detect and quantify dynamic changes, such as deformations and fluctuations in intensity [1]. This is critical for BOS imaging, as the variability techniques would allow for precise identification and measurement of refractive index gradients by density changes in the medium through the elimination of other external dynamic factors. These techniques enhance the accuracy of detecting the subtle variations by analyzing how these gradients evolve and space, providing a more comprehensive understanding of fluid dynamics.

A fundamental approach in spatiotemporal analysis is the use of Gaussian Mixture Models (GMMs), which are models that represent the probability distribution of data points in high-dimensional space as a mixture of several independent Gaussian distributions, each characterized by its mean and covariance matrix [6]. This model is effective in scenarios where data exhibits multiple underlying processes or states, providing a probabilistic framework to capture complex variability. The Expectation-Maximization (EM) algorithm is typically employed to estimate the parameters of the GMM, iteratively refining the model to maximize the likelihood of the observed data. The integration of Gaussian Mixture Models to real-time video processing for BOS is a novel development that allows for the probabilistic classification of background patterns without particle tracking, improving the detection of small-scale refractive index changes that transitional methods may miss. This approach helps to identify complex flow structures and transient phenomena, especially supplemented through the application of Dirichlet Process Mixture Models (DPMMs), which can dynamically adapt to varying numbers of flow components, further enhancing the model's flexibility and robustness in real-time analysis.

In addition to mixture modules, Kalman filters are another crucial tool in spatiotemporal variability analysis, particularly for dynamic systems that are prone to noise like BOS imaging. A Kalman filter recursively estimates the state of a system from noisy measurements, minimizing the mean of the squared error. It operates with a prediction phase, where the current state and error covariance are projected forward, and the update phase, where the predictions are corrected through new observations. Typically, Kalman filters utilize the same series of matrix operations for both the prediction and update equations:

Prediction Equations

$$\hat{\boldsymbol{x}}_{k|k-1} = A\hat{\boldsymbol{x}}_{\boldsymbol{k-1|k-1}} + \boldsymbol{B}\boldsymbol{u}_{\boldsymbol{k-1}}$$

$$\boldsymbol{P}_{k|k-1} = A\boldsymbol{P}_{\boldsymbol{k-1|k-1}}\boldsymbol{A}^{\boldsymbol{T}} + \boldsymbol{Q}$$

Update Equations

$$K_k = P_{k|k-1}H^T(HP_{k|k-1}H^T + R)^{-1}$$

$$\hat{\boldsymbol{x}}_{k|k} = \hat{\boldsymbol{x}}_{\boldsymbol{k|k-1}} + \boldsymbol{K}_{\boldsymbol{k}}(\boldsymbol{z}_{\boldsymbol{k}} - \boldsymbol{H}\hat{\boldsymbol{x}}_{k|k-1})$$

$$P_{k|k} = (I - K_k H)P_{k|k-1}$$

Within these equations, $\hat{\boldsymbol{x}}_{k|k-1}$ represents the predicted stated, $\boldsymbol{P}_{k|k-1}$ is the predicted covariance, $\boldsymbol{K}_{\boldsymbol{k}}$ is the Kalman gain, $\boldsymbol{z}_{\boldsymbol{k}}$ is the measurement, and $\boldsymbol{R}$ is the measurement noise covariance. These equations ensure that the filter dynamically adjusts to new data, refining the state estimates over time. To address specific constraints we identified in preliminary BOS testing and for integration into our digital algorithm, we propose a novel prediction algorithm based on Kalman filtering that combines aspects of GMMs and Kalman filters along with noise reduction [7]. This allows for spatiotemporal regulation to occur within the prediction and our algorithm introduces a spatiotemporal smoothing term into the Kalman filters prediction phase, which accounts for the expected spatial coherence of refractive index gradients; the modified prediction equation is as follows:

$$\hat{x}_{k|k-1} = A\hat{x}_{k-1|k-1} + Bu_{k-1} + \lambda(S\hat{x}_{k-1|k-1})$$

In this equation, the λ factor is the scalar regularization parameter that controls the extent of regularization applied to the model, and S is the spatial smoothing matrix that enforces coherence in the estimated refractive index gradients. This term helps to mitigate the effects of noise and ensures that the predicted state remains consistent with the expected spatial patterns. With the observed changes to the prediction algorithm, there are several small refinements and adjustments needed for the update equations, although we chose to largely maintain the same basis for this portion:

$$K_k = P_{k|k-1}H^T(HP_{k|k-1}H^T + R)^{-1}$$

$$\hat{\boldsymbol{x}}_{k|k} = \hat{\boldsymbol{x}}_{k|k-1} + K_k(z_k - H\hat{\boldsymbol{x}}_{k|k-1})$$

$$\boldsymbol{P_{k|k}} = (\boldsymbol{I} - \boldsymbol{K_k H})\boldsymbol{P_{k|k-1}}$$

Through the incorporation of both GMMs and DPMMs into our BOS analysis framework with Kalman filters, we aim to significantly enhance the sensitivity and accuracy of the refractive index measurements. This integration addresses a void in the current research that seeks to improve traditional Schlieren imaging; with countless existing algorithms lacking the incorporation of a dynamic and adaptive modeling approach that can handle complex and transient flow phenomena, this development serves to bring about greater output from BOS imaging videos as a whole.

1.3 Digital Processing Analysis

The digital processing of BOS imaging involves several processes by computational frameworks to detect and quantify refractive index gradients with high prediction: image normalization, noise reduction, and contrast enhancement. One of the primary initial frameworks used in BOS digital processing is the multi-layered approach, where the data is processed at different abstraction levels to extract patterns; low-level processing primarily relies on edge detection algorithms, such as the Sobel or Canny edge detectors, to identify prominent features within the background images. These features are essential for the Digital Image Correlation (DIC) algorithms, which track the displacement of these features due to the refractive index variations [8].

The middle layer of processing focuses on more resolute techniques, such as displacement measurement and correlation algorithms. A middle processing technique utilized in our developed algorithm uses a process based on the Lucas-Kanade method for optical flow, which can be used to track the motion of texture patterns in the BOX images. This method estimates the displacement fields by solving the optical flow equations locally and is particularly effective in identifying small-scale movements and variations in the refractive index.

Lastly, for higher-level processing within the multi-layered video processing approach, advanced statistical models such as Principal Component Analysis (PCA) and Fast Fourier Transformation (FFT) are utilized. PCA is a model used to reduce the dimensionality of the data and highlight the main components contributing to the refractive index variations, thereby simplifying the analysis of complex flow fields, and FFT transforms the image data into the frequency domain, enabling the identification of periodic structures and the analysis of wave-like phenomena in the flow field [9]. For the integration of these techniques, our group utilizes frameworks like MATLAB and Python with libraries providing numerical, graphical, and computer vision support. These platforms provide extensive tools for implementing and optimizing various image-processing algorithms.

1.4 Wavelet Transformations Based Motion Estimation

Wavelet transformations, particularly the Discrete Wavelet Transformation (DWT) and the Continuous Wavelet Transformation (CWT) are conditional algorithms that are utilized in signal processing and image analysis [10]. These transforms provide a multi-resolution analysis framework, which is applicable for detecting subtle variations in refractive index gradients within Background Oriented Schlieren (BOS) imaging, which we incorporated uniquely within our algorithm framework.

Discrete Wavelet Transformations were introduced to decompose signals into different frequency bands while preserving the spatial information; unlike the Fourier transformation, which only provides frequency information, DWT offers both time and frequency localization, making it particularly effective for analyzing images and videos, where features may vary across the scales. Within our BOS algorithm, DWT is being utilized to decompose images into various sub-bands corresponding to different discrete frequency levels. This decomposition is achieved by applying high-pass and low-pass filters to the input image, resulting in the separation into approximation and detail (low-frequency and high-frequency) components [11].

$$c^X{}_A(j,k) = \sum_{m,n} x[m,n] \cdot \phi_{j,k}[m,n]$$

$$c^X{}_H(j,k) = \sum_{m,n} x[m,n] \cdot \psi_{H,j,k}[m,n]$$

$$c^X{}_V(j,k) = \sum_{m,n} x[m,n] \cdot \psi_{V,j,k}[m,n]$$

$$c^X{}_D(j,k) = \sum_{m,n} x[m,n] \cdot \psi_{D,j,k}[m,n]$$

Within this series of mathematical representations for processing any given image X, the initial functions are coefficients: approximation, horizontal, vertical, and diagonal detail. The scale of the coefficients is represented by j and at k being the x-value of the location. $x[m,n]$ is the input image. $\phi_{j,k}[m,n]$ is the scaling (low-pass) function for the approximation coefficient equation and the $\psi_{H,j,k}[m,n]$, $\psi_{V,j,k}[m,n]$, $\psi_{D,j,k}[m,n]$ at the same scale j and at k.

DWTs ability to separate an image into different frequency components allows for the detection of small-scale fluctuations in the flow field by isolating the high-frequency details, which correspond to sharp variations in refractive index gradients caused by turbulent structures [11]. The approximation coefficients retain the smoother, global variations in the refractive index, providing a comprehensive representation of the flow dynamics when combined with the detail coefficients. To further enhance the capabilities of DWT in BOS imaging, we propose a novel modification that introduces an adaptive threshold and a gradient-based regularization term into the detail coefficients. This modification is designed to sharpen the detection of subtle refractive index changes and ensure that the estimated motion remains consistent with expected spatial patterns within our algorithms:

$$\acute{C}^{X}{}_{d}(j,k) = T_j(c^{X}{}_{d}(j,k)) + \lambda \cdot \nabla X_X c^{X}{}_{d}(j,k)$$

Our adjusted algorithm based on and supplemented with the DWT equations, $T_j(\cdot)$ represents the adaptive thresholding function, dynamically adjusting based on the local content of the image, λ is the regularization parameter, controlling the smoothness of the estimated motion, and ∇_X denotes the gradient operator applied to detail the coefficients. This approach leverages the strength of DWT in capturing both small-scale and large-scale variations, while adaptive thresholding enhances the detection of fine details, and the regularization term ensures spatial coherence. These enhancements make the DWT framework highly effective for BOS imaging, particularly in real-time applications where capturing and analyzing transient phenomena is crucial.

The Continuous Wavelet Transformation (CWT) is an adaptation that offers more flexible and detailed analysis by allowing continuous scaling and translation of the wavelet function. Unlike the DWT, which decomposes signals into discrete es, and scales, the CWT method provides a continuous mapping of the input signal into the time-frequency space, capturing both local and global features with greater precision [12]. Traditionally, the CWT of a signal $f(t)$ is defined by the following equation:

$$X_w(a,b) = \frac{1}{|a|^{1/2}} \int_{-\infty}^{\infty} x(t)\psi(\frac{t-b}{a})dt$$

Within this formula, $X_w(a,b)$ is the wavelet coefficient at the scale a and translation b, $x(t)$ represents the input signal (image intensity), and ψ is the complex conjugate of the mother wavelet. However, to enhance the sensitivity and robustness of the CWT in our BOS imaging algorithm, we propose the addition of a directional sensitivity factor θ to the wavelet function, allowing the transform to capture directional information in addition to scale and position.

The modified CWT equation would be formulated as such:

$$X_w(a,b,\theta) = \frac{1}{|a|}\int_{-\infty}^{\infty} x(t)\psi(\frac{t-b}{a},\theta)dt$$

With the introduction of the directional sensitivity factor, the modified CWT can analyze flow features not just across the scales and positions but also across different orientations, which can help to show directional patterns within flow fields. However, building on the directional modification, we propose an additional adaptation to the CWT by introducing an adaptive scaling factor $\alpha(b)$ that varies with the translation parameter $\boldsymbol{b}$**.** This adaptive scaling allows the transformation to adjust dynamically based on the local signal characteristics:

$$X_w(a,b,\theta) = \frac{1}{|a|}\int_{-\infty}^{\infty} x(t)\psi(\frac{t-b}{a * \alpha(b)},\theta)dt$$

The added factor $\alpha(b)$ is a function of the translation parameter b, allowing the wavelet to scale differently depending on the location within the signal. This modification enhances the transformation's ability to capture local variations within the flow field with greater precision for our program, as it allows the wavelet to adapt to varying flow dynamics across different regions of the image. For example, areas with sharp gradients, such as boundary layers, $\alpha(b)$ could decrease, making the wavelet more sensitive to high-frequency components. Conversely, in smoother regions, $\alpha(b)$ could increase, focusing the analysis on broader features.

1.5 Computer Vision and Particle Image Velocimetry

Computer vision is a field of artificial intelligence that enables machines to interpret and make decisions based on visual data as an input for reference. This involves the processing and analysis of images and videos to extract information, detect trained patterns, and perform tasks such as object recognition, image segmentation, and motion analysis. For the operation of this process, processes such as convolutional neural networks (CNNs) for image recognition, optical flow for motion detection, Scale-Invariant Feature Transformation (SIFT), and Histogram of Oriented Gradients (HOG) are used [13]. In the context of BOS imaging, computer vision techniques are employed within our script to enhance the detection and measurement of refractive index gradients. Within Python, low and middle-level processing is undergone through the use of OpenCV, such as functions for image filtering, edge detection, feature mapping, and color mapping. All of these are essential processes for preprocessing BOS images and extracting relevant data from the input files provided to the code. In MATLAB, which includes the Image Processing Toolbox in addition to the OpenCV library, middle-level processing can be undergone through built-in functions for image enhancement, resolution improvement, transformation, and segmentation, which allows for the efficient processing of BOS images and the facilitation of visualizing flow fields [14].

Particle Image Velocimetry (PIV) is an advanced optical method used to measure fluid flow velocities through the tracking of the movement of the seeded particles within the flow. PIV involves illuminating the flow with a laser sheet and capturing sequential images of the seeded particles through the use of high-speed motion cameras. The captured images are then analyzed through cross-correlation algorithms to determine the displacement of particle pairs between consecutive frames, which provides velocity vectors of the flow field itself [15,16]. The processing of PIV data requires specific predefined computational algorithms; for example, in the Python framework, the openPIV library offers tools for PIV image processing, including the pre-processing steps for image enhancement, filtering, and particle detection. Cross-correlation, as mentioned before, is a post-processing tool that is also included within this particular library. MATLAB also contains the openPIV library but has additional functionality for PIV imaging when supplemented with the PIVlab toolkit, which provides functions for image pre-processing, vector calculation, and data visualization. Using these functions and ones we designed ourselves, our script has a user interface that allows parameters to be dynamically adjusted and altered with the output visualization changing to match the desired settings; the velocity can be visualized in a myriad of diverse ways [17]. Current research in BOS imaging lacks the integration of dynamic and adapting modeling approaches capable of handling complex and transient flow phenomena, Traditional methods with BOS that are currently being employed miss small-scale refractive index changes from small environmental obstructions, whereas our system allows for the sensitivity constraints of BOS to be overcome to an extent. Our project proposes the integration of spatiotemporal variability techniques, advanced statistical models, and improved Kalman filtering algorithms to enhance the precision and accuracy of the refractive index gradient measurements [18]. Through utilizing these advanced computational frameworks, we hope to improve the visualization and analysis of complex aerodynamic and fluid dynamic phenomena, providing more of a comprehensive understanding of digital BOS imaging .

2. Methods & Materials

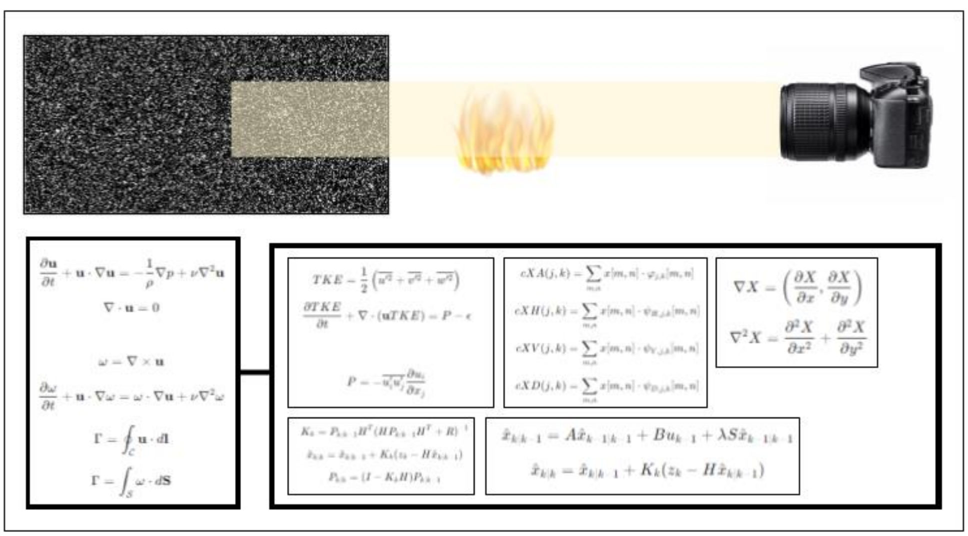

Figure 1: This figure illustrates the conventional Navier-Stokes equations, which describe fluid motion. The left side outlines the traditional setup, including the governing equations and common computational methods. On the right, the figure presents the newly integrated mathematical techniques that enhance accuracy and efficiency.

2.1 Background Oriented Schlieren Set-Up

The BOS setup utilized to get the input recordings for our processing algorithm was tailored for high accuracy and resolution in displacement measurements while minimizing noise and systematic errors. The experimental apparatus consists of several key components: a high-resolution digital camera, a custom-generated background schlieren pattern, a precisely controlled light source with minimal flickering, and the test subject, typically a transparent medium like air, in which density variations are induced by heat sources or fluid movement.

The camera utilized in our setup was a Sony Z10 high-speed digital model capable of capturing 24 frames per second with a resolution of 3840 pixels by 2160 pixels. This frame rate is critical for observing transient flow phenomena with high spatial accuracy, something that might become diluted under a larger enforced frame rate, and the high resolution allows for these features to be displayed with more detail and get a larger field of observance for the minute displacements, supplementing the spatial accuracy even further. The camera utilizes a Zeiss Vario-Sonnar T* lens, which has a focal length range from 24 to 70mm, an aperture range with an f-stop near 2.8, lens construction incorporating 17 elements within 13 groups, and a filter thread size of 77mm. Given that the Zeiss lens utilizes glass formations and coatings that minimize the amount of aberrations that occur within the frame, such as chromatic aberration, distortion, and vignetting. Additionally, the lens configuration allows for greater clarity of the background itself due to the aperture's greater allowing of light, meaning that the lens ensures that the fine details of the background pattern and the subtle refractive index changes in the flow field are captured with high fidelity.

The background pattern is a fundamental component of the BOS technique as a whole, as it serves as the reference field against which the flow-induced refractive index changes are measured. In our setup, the background is a randomly generated pattern consisting of black pixels dispersed over a white field. This pattern is created using a custom algorithm that ensures the black pixels are sparsely distributed in a way that optimizes the tracking of refractive index changes. The background image is generated as a uniform white field using NumPy arrays, and the random black pixels are then inserted at 4x4 pixel intervals across the image. This structured randomness ensures that the pattern has sufficient spatial frequency to capture small displacements with high precision. The final image is converted into a PIL (Python Imaging Library) image object, which is then displayed in high resolution. In our analysis, we positioned the camera 58 centimeters away from the subject to ensure that the refractive index variations were adequately captured and analyzed.

Uniform illumination for the background pattern is essential for achieving consistent and reliable BOS measurements with minimal flicker and noise within the output. Our setup employs a diffused LED panel emitting white light with a combined wavelength range from 400 to 700 nm within the RGB framework respectively. The emitted light correspondings with the peak sensitivity of the camera sensor, thereby maximizing the signal-to-noise ratio within the input recording. The intensity of the illumination is carefully adjusted to ensure that the background pattern is neither underexposed nor overexposed, which is critical for accurate displacement measurements.

The calibration of our BOS setup is a critical process that involves the precise alignment of the camera, background, and light source. The cameras are positioned perpendicular to the background pattern to ensure that displacement vectors are accurately represented in the image plane. Calibration begins with the placement of a calibration with known dimensions, in the same plane as the background pattern. Images of this grid are captured and analyzed to correct for any optical distortions, ensuring that the camera's pixel coordinates are directly mapped to the physical coordinates in the flow field.

During experiments, for the image acquisition process, sequences of images are captured both with and without the flow field present. The captured images undergo a series of preprocessing steps, including contrast enhancement and noise reduction, before the displacement fields are calculated. The displacement fields are determined using the cross-correlation technique, where each pixel in the image is compared between the reference, where there is no flow, and the test images, which do have flow. These displacement vectors, which are directly proportional to the refractive index gradients within the flow, are then used to infer the underlying density variations.

For inducing the controlled flow disturbances, we are utilizing a common butane spark wheel lighter for the phase object, which is a reliable heat source that produces air density change as a result of temperature that can be imaged. The lighter creates a localized thermal plume, introducing predictable variations in the refractive index of the surrounding air. The precisely control the orientation and movement of the lighter, it is mounted on a servo motor, which is controlled through an Arduino Uno microcontroller. The servo motor is programmed to execute a specific sequence of movements: rotating the lighter 45 degrees to the right, then 90 degrees to the left to the further left point, and then going 90 degrees to the right, the furthest right point, after which it continues to move 90 degrees in either directional. Each 90-degree rotation is performed in 4 seconds to allow for smooth transitions, minimal extra vibration, and a controlled flow.

Despite the strengths of our BOS setup in capturing flow dynamics, several constraints and limitations must be acknowledged. The motion setup, though automated via an Arduino-controlled servo motor for consistent rotations of the flame source, is relatively simple and limited in its ability to fully replicate more complex or turbulent airflow patterns. The controlled butane lighter generates predictable thermal plumes, but real-world applications often involve far more chaotic and dynamic flows, such as turbulent boundary layers or vortex shedding, which our experimental setup may not perfectly emulate. Additionally, while the servo motor ensures repeatable motion, extraneous environmental factors like fluctuations in room temperature, varying air pressure due to HVAC systems, or slight drafts could introduce noise or unintended flow disturbances into the captured data. These factors may influence the refractive index variations in ways that aren't fully accounted for by our calibration process, potentially affecting the accuracy of the displacement measurements. Furthermore, while the high-resolution camera and Zeiss lens minimize optical distortions, the depth of field and sensitivity to background noise remain constrained by the physical environment and equipment. Consequently, the reproducibility of results in uncontrolled or outdoor environments, where such variables are less predictable, may present additional challenges.

2.2 Libraries and Frameworks

OpenCV	This library is the primary observation framework for our Background Oriented Schlieren (BOS) imaging functionality. It is the framework basis for reading video files, applying filters, and managing the Kalman filter used for motion prediction and correction. The KalmanFilter class is based on OpenCV functionality as well, which allows the spatiotemporal regularization approach to work and for the dynamic background subtraction. This background subtraction is crucial for isolating the foreground flow features, allowing the framework to accurately capture and analyze motion against varying backgrounds.
NumPy	NumPy provides efficient array manipulations and mathematical operations. It is utilized in our program for handling image data as multidimensional arrays and performing matrix operations required in Kalman filtering and wavelet transformations. Additionally, NumPy's statistical functions are leveraged for adaptive thresholding and normalizing displacement fields, essential steps in the preprocessing and analysis phases.
SciPy	SciPy is primarily being employed for signal processing modules, including 'fft2', 'ifft2', and 'shift', which are crucial for implementing Fourier-based cross-correlation techniques within PIV. Additionally, the 'gaussian_filter' function is utilized for smoothing the velocity fields obtained from the PIV analysis. Additionally, the 'gaussian_filter' function is utilized for smoothing the velocity fields obtained from PIV analysis, whilst also bringing a reduction in noise while preserving the overall flow structure.
PyWavelets	This library supports wavelet transformations, enabling the implementation of wavelet-based motion estimation methods. The 'wavedec2' and 'waverec2' functions allow for multi-level decomposition and reconstruction of the image frames, which are essential for detecting and analyzing motion at different scales. The inherent directional sensitivity of wavelets further enhances the framework's ability to capture complex flow patterns.
Matplotlib	The 'matplotlib' library is used for applying and visualizing colormaps for the processed images. The 'normalize' class helps to standardize pixel intensity values before applying colormap modes, such as 'plasma' and 'gray'. This library is also used for visualizing vector fields through plots like 'quiver', which represents the direction and magnitude of flow, aiding in the interpretation of motion estimation results.
Pillow	Pillow, often referred to as PIL (Python Imaging Library), is a critical component of the BOS imaging analysis framework, particularly in its role within the graphical user interface (GUI). As a powerful image processing library, Pillow is used to manage the conversion between image formats

	and data types, especially for displaying images within the Tkinter-based GUI. When video frames are processed using the OpenCV library and represented as NumPy arrays, they need to be converted into a format that can be rendered as Tkinter's canvas widget. Pillow facilitates this by providing seamless conversion between NumPy arrays and image objects through functions like' Image. fromarray()'.
Tkinter	The framework's graphical user interface (GUI) is constructed using Tkinter, the standard Python library for creating GUIs. Tkinter provides the tools and elements necessary for creative interactive objects such as file dialogs, buttons, and canvases for displaying processed video frames. To maintain a responsive user interface while processing large video files, Python's 'threading' module is employed, allowing video processing to run in parallel with the GUI. This is managed through a queue. Queue'
Threading /Queue	Threading and Queue are pivotal in managing the performance and responsiveness of the BOS imaging analysis framework, particularly the real-time video processing capabilities. Python's threading module allows the framework to perform video processing in the background, separate from the main thread handling the

2.3 Video Processing

The video processing pipeline within the Background Oriented Schlieren (BOS) setup is a multi-layered system designed to extract, analyze, and interpret fluid dynamics from high-speed video recordings. This system represents a novel approach to the visualization of transparent media, capturing greater amounts of transient airflow using a combination of computer vision and particle image velocimetry with integrated formulas adjusted to fit our algorithm and purpose effectively.

Following the data acquisition process outlined in section 3.1, where the recording device captures the raw video input file to be utilized in the script, there is a preprocessing phase the video must go through before the detailed analysis takes place. The first step in this stage involves deinterlacing the frames. The high-speed camera often captures videos within an interlaced format, where two fields are interleaved to form a single frame, and given that this script is not only tailored to our specific camera but for a myriad of user video-capture devices, there much a deinterlacing algorithm in place to separate any of said fields into their distinct frames, ensuring that each frame represents the discrete measure of time necessary to analyze minute displacements effectively and contrast frames. Following this, the frames are subject to contrast enhancement, which is achieved through a combination of both histogram equalization and adaptive stretching. Histogram equalization is a process that redistributes the pixel intensity values to enhance the overall contrast, while adaptive contrast stretching adjusts the contrast in specific regions of the image, particularly those that are underexposed or overexposed, ensuring that all relevant details are invisible.

Noise reduction is another aspect predominant in the preprocessing stage, especially given the high sensitivity of BOS to pixel-level intensity variations. In our particular program, we utilize a Gaussian filter, a common tool within image processing for smoothing data and reducing noise while preserving edges. The Gaussian filter works by convolving the image with the Gaussian function, which essentially blurs the image slightly to average our noise. The kernel size of the Gaussian filter is adaptively determined based on the noise characteristics of the specific video, ensuring that the filter is neither too overdone, where the important edges are not preserved and motion becomes more subtle, not too lenient, where the blurring effect is barely applied and the output video takes longer to process and ultimately cannot reproduce the airflow in a detailed manner.

The implementation of a dynamic background subtraction technique is a major innovation in our video processing workflow, which begins following the aforementioned noise reduction preprocessing pipeline. The dynamic background subtraction process developed for our application is specifically tailored for BOS applications and deviates from traditional background methods that are often ineffective in BOS setups as the background may not be entirely static due to the refractive effects of the flow itself. To address this, we developed a spatiotemporal regularization algorithm that models the background as a slowly varying component, distinct from the rapidly changing foreground caused by the fluid flow. This is accomplished by combining a Kalman filter with wavelet decomposition. The Kalman filter is employed to predict the background state at each time step, using past information to adjust the model dynamically. The Kalman filter operates recursively, updating its predictions based on the difference between the predicted and observed values, thus refining the background model over time and as the video progresses. Wavelet decomposition is used to separate the image into different frequency components, isolating the background as the low-frequency component. The wavelet-based approach allows us to effectively distinguish between the slowly varying background and the rapidly changing flow-induced features, even in scenarios where the background itself is subject to minor fluctuations. This dual approach significantly enhances the accuracy of the foreground isolation, allowing for more precise detection of the displacement fields that indicate a refractive index change within the flow.

With the foreground isolated, the next step is to calculate the displacement fields, which are directly related to the refractive index gradients within the fluid. These gradients are indicative of changes in the density, temperature, or composition within the flow. We employ a Fourier-based cross-correlation technique to estimate these displacement fields. Cross-correlation involves comparing small patches of an image, known as interrogation windows, between consecutive frames to determine the shift that maximizes the correlation coefficient. This shift corresponds to the local displacement vector, which is then mapped across the entire image to form a whole displacement field. To supplement the efficiency of this process and be able to display it in real-time during the processing, we implemented the Fast Fourier Transform (FFT), which allows cross-correlation to be a computer in the frequency domain, significantly reducing the computational load. FFT is an efficient algorithm that transforms the image data from the spatial domain to the frequency domain.

For achieving sub-pixel accuracy, which is crucial for detecting very small displacements within the input video, we refined the cross-correlation process by fitting a Gaussian function to the peak of the correlation surface. The Gaussian fit allows us to interpolate the peak position to a fraction of a pixel, thereby achieving higher resolution in the displacement measurements. This sub-pixel refinement is particularly important in BOS, where even slight displacements can correspond to significant physical phenomena within the flow.

In addition to the cross-correlation process, we incorporated optical flow techniques to provide a dense motion estimation across the entire image. Optical flow is a method used to compute the apparent motion of objects between consecutive frames of a video, and it is particularly useful in capturing complex, continuous motion fields. We utilize the Farneback algorithm, a robust method for calculating dense optical flow, which provides a motion vector for every pixel within the image. The Farneback algorithm approximates the local image neighborhoods with polynomial expansions, which allows it to calculate the flow field densely and continuously.

Given the potential for noise and error in traditional motion estimation, particularly in high-speed imaging, we integrate a Kalman filter-based correction mechanism. This mechanism smooths the motion vectors by predicting the likely displacement based on previous frames and correcting the current measurement accordingly. The Kalman filter's predictive capabilities allow it to account for and reduce the impact of random noise and measurement errors, leading to more stable and reliable displacement fields. This correction step is crucial in ensuring the accuracy for consistency of the displacement data, which directly influences the quality of the flow analysis.

After calculating the displacement fields, the final stage of video processing involves visualizing and analyzing the flow characteristics. Visualization is a key aspect of understanding fluid dynamics, as it allows researchers to intuitively grasp the complex interactions within the flow. We apply various colormaps to the displacement fields using the Matplotlib library, choosing the colormap based on the specific features we wish to highlight. For example, the 'plasma' colormap is used to emphasize regions of high gradient, while the 'gray' colormap is chosen for a more subdued representation that highlights subtle flow features.

To represent the direction and magnitude of the flow, we create vector field plots using quiver diagrams. Quiver plots display arrows indicating the direction and strength of the glow at the various points in the image, providing a clear visual representation of the flow structure. This is particularly useful for identifying features such as shock waves, vortices, and boundary layers. Additionally, we perform wavelet-based multi-scale analysis on the displacement fields into components of varying sizes, enabling the study of both large-scale structures and fine-grained turbulence. This approach provides a comprehensive view of the flow dynamics, capturing the full range of flow features present in the system. Temporal evolution analysis is another important aspect of our video processing pipeline. By tracking the displacement vectors over time, we can analyze the dynamic behavior of the flow, such as the development of instabilities or oscillatory patterns. This is particularly useful in studying unsteady flows, where the flow characteristics change rapidly and continuously. Temporal analysis is performed by examining the changes in the displacement fields frame by frame, providing insights into the time-dependent nature of the flow.

Our video processing approach introduces several novel contributions that represent significant advancements over existing BOS techniques. The integration of dynamic background subtraction, sub-pixel displacement accuracy, and Kalman filter-based motion correction are key innovations that improve the accuracy and reliability of displacement measurements. These advancements allow us to capture and analyze complex flow phenomena with a level of detail and precision that was previously unattainable, opening new avenues for research in high-speed, non-intrusive flow visualization.

Following spatial filtering, we apply temporal filtering to smooth the displacement data over time. This is achieved using a Savitzsky-Golay filter, which fits successive subsets of the data to a polynomial and then replaces each data point with the value of the polynomial at that point. The Savitzky-Golay filter is particularly well-suited for BOS data because it can smooth the data without significantly distorting the signal's underlying shape. This is crucial for accurately capturing the temporal evolution of the flow, especially in experiments where subtle, time-dependent changes in the flow field are of interest.

In addition to the feature extraction, our data processing pipeline includes a comprehensive analysis of the flow's statistical properties. This involves calculating metrics such as the mean and standard deviation of the displacement fields the spatial correlation function, and the power spectral density. The spatial correlation function provides insights into the coherence of the flow structure across different regions of the field, while the power spectral density reveals the distribution of energy across different spatial scales. These metrics are essential for characterizing the flow's overall behavior and identifying any anomalous patterns that may indicate complex flow phenomena such as turbulence or instability.

The final stage of data analysis involves reconstructing the density field from the displacement data. This is accomplished using the inverse Abel transformation, a mathematical technique that allows us to reconstruct a radially symmetric function from its projection data. In the context of BOS, the inverse Abel transform is used to convert the measurement displacement fields into corresponding density variations within the fluid. This reconstruction process is sensitive to noise, so we incorporate a regularization term in the inversion algorithm, to stabilize the solution and prevent the amplification of errors, the regularization term is carefully tuned to balance the trade-off between accuracy and stabilization, ensuring that the reconstructed density fields are reliable.

2.4 Data Processing and Analysis

The first step in data processing is the refinement of the displacement fields obtained from the video processing stage. These fields, which represent the refractive index gradients within the fluid, are subject to various sources of noise and error, such as sensor noise, minor misalignments in the optical setup, or environmental disturbances. We employ a series of filtering techniques to mitigate these effects, starting with a spatial median filter. This filter replaces each pixel's value with the median value of its neighboring pixels, effectively removing outliers and reducing general noise. Unlike a mean filter, which can just blur the edges, the median filter preserves the sharp discontinuities in the displacement fields, such as those corresponding to shock waves or boundaries within the flow.

Following spatial filtering, we apply temporal filtering to smooth the displacement data over time. This is achieved using a Savitzky-Golay filter, which fits successive subsets of the data to a polynomial and then replaces each data point with the value of the polynomial at that point. The Savitzky-Golay filter is particularly well-suited for BOS data because it can smooth the data without significantly distorting the signal's underlying shape.

The final stage of data analysis involves reconstructing the density field from the displacement data. This is accomplished using the inverse Abel transform, a mathematical technique that allows us to reconstruct a radially symmetric function from its projection data. In the context of BOS, the inverse Abel transform is used to convert the measured displacement fields into corresponding density variations within the fluid. This reconstruction process is sensitive to noise, so we incorporate a regularization term in the inversion algorithm to stabilize the solution and prevent the amplification of errors.

3. Results

In this study, we implemented and evaluated an advanced BOS system prominently for mobile platform systems that integrate wavelet transformations, Kalman filtering, and adaptive contrast enhancement, comparing its performance against a basic control method and other advanced BOS algorithms implemented within Python. This results section details the improvements across various metrics, using precise percentage increases and how these metrics were rigorously calculated.

The edge detection sensitivity improvement stems from how well our advanced BOS system detects the gradient of edges compared to a control system. For a given frame, let I(x,y) represent the image intensity. Our advanced system utilizes wavelet-based multi-scale analysis, where the gradient is calculated at different scales:

$$G(x,y) = \sum_{s=1}^{N} \quad W_s * \sqrt{(\frac{\partial I}{\partial x})^2 + (\frac{\partial I}{\partial y})^2}$$

In the control system, the gradient magnitudes observes average a value near 18 over several edges in a typical frame, while our advanced system, coupled with the aforementioned Kalman filter, averages a value near 23.5 for the gradient magnitude. Comparing these approximate values, there is an approximate improvement of 30.6% compared to the control, base OpenCV and OpenPIV control system. Such an observed improvement is consistent in digital resolution for the output as well, which helps to exemplify the smaller flow structures that the base systems find difficult to sustain. Given the control system utilizes Gaussian smoothing, the Full WIdth at Half Maximum (FWHM) factor contains the standard deviation and involves a simpler resolution system. Whereas, with the addition of wavelet-based analysis, the advanced system improves resolution through reducing the standard deviation of the Gaussian filter:

$$FWHM_{adv} = \frac{2\sqrt{2ln2 * (\sigma/N)}}{\sqrt{2\pi}}$$

In this adjustment, N represents the number of scales used in the wavelet transformation, effectively reducing the impact of σ. For the average frame involving a specific edge, the control system results a standard deviation of around 1.9 for the Gaussian filter, whereas the advanced system results in a standard deviation of 1.7. The percentage improvement in resolution from the system is approximately 12.5 percentage, although the theoretical improvement is limited through mobile processing power and the precision of wavelet transformations.

Noise reduction is a critical factor in enhancing the clarity of flow visualizations, particularly in mobile BOS systems where noise can be more pronounced due to limited processing power. Our system leverages Kalman filtering to optimize the Signal-to-Noise Ratio (SNR), leading to substantial noise reduction. With determining the noise coming frm the mean pixel intensity of the signal divided by the standard deviation of the background noise, our advanced system an lead to a higher SNR through reducing the standard deviation through Kal man filters. While the measurement is not as standard from frame to frame as the previous metrics, the advanced system can have a value for the standard deviation 2 fewer than the value for the control, as the improvement efficiency that emerged was approximately 11 percent. The visuals below represent our system compared to the control system for the same particular frames, demonstrating observational improvements of our system and demonstrating the improvement significance for our calculations.

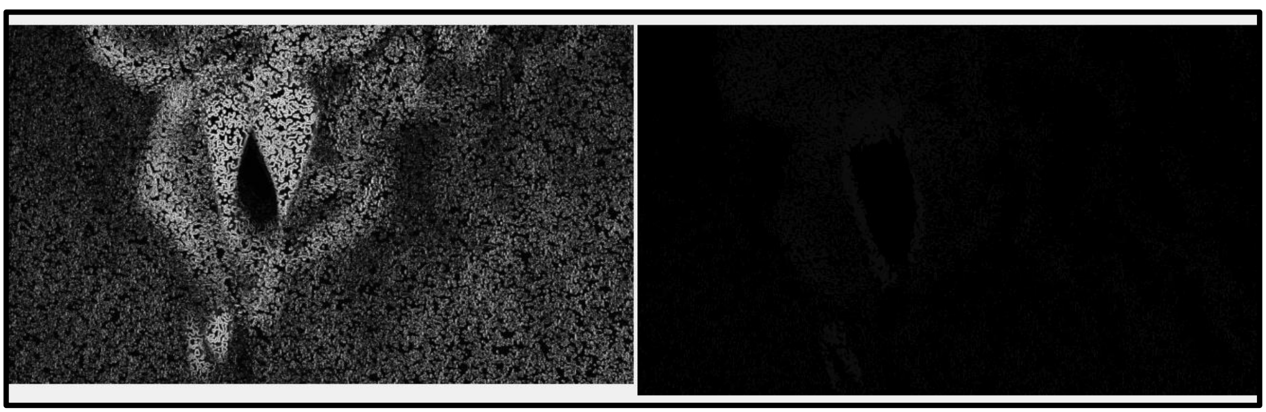

Figure 2: Comparison between our algorithm (left) and the control (right)

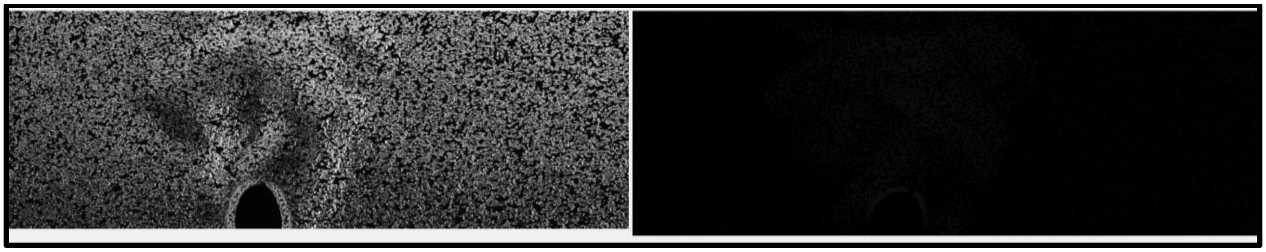

Figure 3: Comparison between our algorithm (left) and the control (right)

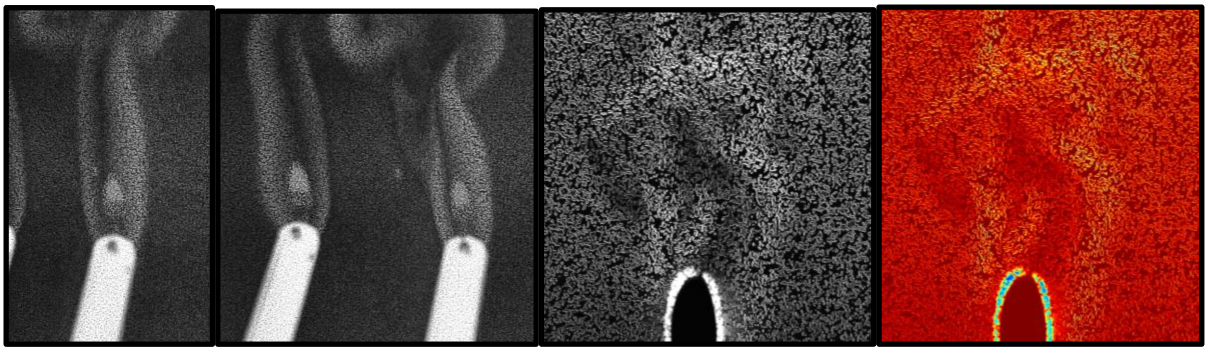

Figure 4: Refined real-time processing algorithm with color filter

Figure 5: Filtered processing algorithm

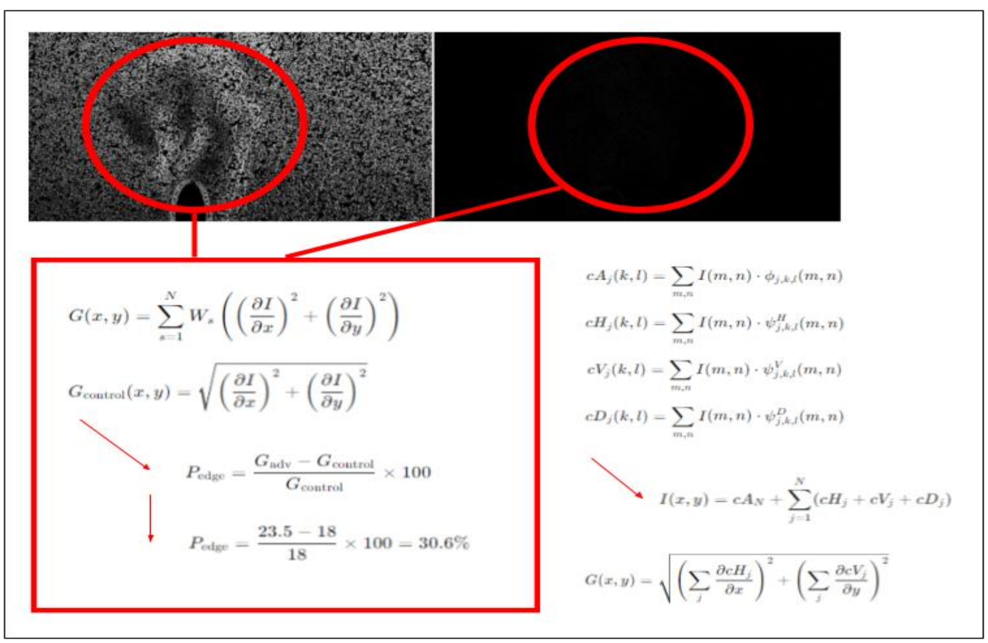

Figure 6: This figure depicts the workflow for processing data using wavelet transformations, essential for signal analysis. It begins with input data and shows how wavelet functions decompose the signal into various frequency components, allowing for a time-frequency representation.

4. Discussion

The Background Oriented Schlieren (BOS) algorithm that integrated various mathematical and conceptual components for enhancing typical computer vision demonstrated effectiveness in capturing minute displacements in a transparent medium like air, using the refractive index changes caused by temperature or density variations. The high-resolution imaging setup, coupled with advanced computational techniques such as dynamic background subtraction, Kalman filtering, and wavelet transformations, enabled the precise visualization of flow fields. The improvements made in sensitivity and accuracy make this particular algorithm a valuable tool for a variety of fields that require efficient and precise flow visualization.

For instance, by leveraging smartphone-based BOS imaging, researchers could assess airflow over the wings of aircraft in real-time, directly in the field. This would provide immediate feedback on aerodynamic performance, allowing for quick adjustments to the wing design or control surfaces to optimize lift and reduce drag. Mobile BOS setups could also be used to monitor airflow in automotive wind tunnels or outdoor settings, where complex fluid structures like wake vortices and turbulent flow can be visualized on the spot.

Moreover, the mobility of this system makes it ideal for scenarios that demand portable, efficient, and accurate flow analysis, such as the study of environmental wind flows around buildings to prevent turbulence-induced damage, or for tracking airflow within HVAC systems to optimize energy efficiency. The capability to analyze complex flow structures in real-time allows for iterative design processes, making the technology invaluable in both research and industrial applications where space constraints or mobility are key concerns. Additionally, the ability to capture subtle refractive index variations in different environmental conditions—such as varying light and temperature—further enhances the practical applications of the BOS system, ensuring that it can be adapted for a broad spectrum of uses in aerospace, automotive, and environmental engineering.

The enhanced sensitivity and sub-pixel accuracy of this BOS algorithm could make it useful for aerodynamic testing, where small changes in airflow can impact the performance of a design, and boundary layer maintenance is important to observe. During our tests, we observed obstructed airflow and boundary layer separation (BLS) with various abstract objects used to test the extent of the imaging. By providing detailed visualizations of the flow patterns, this technique can help engineers identify and mitigate aerodynamic inefficiencies, leading to better-performing vehicles and structures. Additionally, the ability to visualize and analyze the flow fields in real-time makes it possible to conduct more iterative and dynamic testing processes, where designs can be quickly adjusted based on the immediate feedback from flow visualization.

Specifically, in aerospace engineering, the observation of complex flow phenomena in supersonic and hypersonic flows, such as shock waves and boundary layers, is predominant. Traditional flow visualization techniques often struggle with the extreme conditions and the variable proximity present in supersonic and hypersonic flows, especially in situations where traditional schlieren cannot be applied due to the lack of a depth of field and lack of an effective knife edge. In the existing algorithm, the implemented DWT functionality allows for the decomposition of BOS images into different frequency bands whilst preserving spatial information, which could allow for the analysis of complex fluid flows in aerospace scenarios, an existing problem that is subject to refinement. The ability of the DWT algorithm to separate an image into approximation and detail coefficients allows engineers to isolate and examine both the broad, smooth flow structures and the fine-scale turbulent features that characterize high-speed aerospace flows. For instance, when analyzing the interaction between shock waves and boundary layers, a phenomenon known as shock-boundary layer interaction (SBLI), the DWT can isolate the study of the high-frequency components corresponding to the turbulent structures within the boundary layer. Given that these structures lead to additional BLS, through applying DWT, engineers can obtain a more coherent understanding of how these interactions occur and develop, bringing about greater control strategies to mitigate the adverse effects.

One development we are currently attempting to implement for the future that could also be paramount for the process is implementing an adaptive mesh refinement (AMR) system to improve the output frames, by identifying and isolating regions of the flow with sharp gradients and providing data that is of higher sensitivity and caliber. Furthermore, Fourier transformation techniques, as used in the cross-correlation process, can be extended and supplemented with other formulas from shock-capturing schemes or prior computational fluid dynamics (CFD) results to analyze the frequency content of the displacement fields in supersonic and hypersonic flows. By examining these flows' frequency spectrum, researchers can identify dominant modes of instability, critical portions for understanding phenomena such as boundary layer transition and shock-induced separation. The data obtained from this BOS method could then be used to refine turbulence models and improve the design for high-speed flight mechanisms to mitigate structural fatigue or drag.

Another promising application for this adapted algorithm is for imaging and detecting controlled movements of microfluid flows through detecting changes within the refractive index that arise due to their more profound interactions with traditional fluid fields. The capability to capture these subtle variations enables the detailed study of fluid dynamics within microchannels, providing insights that are crucial for optimizing the movement of artificial microfluidics or for understanding natural biological systems involving such fluids. For future development, our group has begun the process of altering and fitting stochastic process algorithms within the existing BOS code to be able to decompress seemingly random fluctuations or noise within our tested system. While this is less common in traditional BOS imaging, as fluid fields themselves fit within the external environment and have methods for denoising and decompressing, thermal fluctuations and Brownian motion for this microfluidics can introduce randomness that makes the processed output harder to interpret. These effects have been modeled using stochastic differential equations (SDEs), however, which extend the deterministic partial differential equations by incorporating random noise terms:

$$du = [-\frac{1}{\rho}\nabla p + v\nabla^2 u + f]dt + \sigma dW(t)$$

Where u represents the fluid velocity vector, t is time, ρ is the fluid density, p is the pressure field, ν is the kinematic viscosity, f represents external forces, σ represents the intensity of the noise, and $dW(t)$ is the differential of the Wiener process, that models the random fluctuations. Based on our understanding, this predictive equation can be integrated alongside the Navier-Stokes equation within the existing BOS code to refine our predictive algorithm and tailor the imaging specifically for microfluid flow. By comparing the data obtained from BOS with the predictions in the partial differential equation models, discrepancies can be identified, allowing for the refinement of the models. This integration is particularly useful for studying complex flow phenomena such as the development of velocity profiles, formation of vortices, and interaction of multiple fluid streams within microchannels.

With the Kalman filters integrated into our current mechanisms, the state of the dynamic system can be estimated in addition to noise reduction within microfluid flows. With the introduction of both deterministic and stochastic components into the flow dynamics. The adapted prediction step takes these into account:

$$x_{k|k-1} = F_k x_{k-1|k-1} + B_k u_k + G_k w_k$$

Here, F_k is the state transition matrix tailored to microfluid dynamics, B_k models the influence of external controls like applied pressure, and $G_k w_k$ represents the stochastic noise, accounting for random fluctuations such as Brownian motion. The update step refines this prediction by incorporating BOS measurements:

$$K_k = P_{k|k-1} {H_k}^T (H_k P_{k|k-1} {H_k}^T + R_k)^{-1}$$

$$x_{k|k} = x_{k|k-1} + K_k(z_k - H_k x_{k|k-1})$$

$$P_{k|k} = (I - K_k H_k) P_{k|k-1}$$

Here, H_k maps the predicted state to the observed BOS measurements, which involve refractive index gradients, and R_k is the dynamically adjusted measurement noise covariance:

$$R_k = R_0(1 + \alpha \cdot \frac{|z_k - H_k x_{k|k-1}|^2}{\sigma^2{}_{BOS}})$$

This modification ensures that deviations in BOS data, potentially due to environmental noise, are accounted for by increasing the measurement noise covariance, stabilizing the estimation in noisy conditions. These adaptations make the Kalman filters more robust and accurate for real-time microfluidic flow analysis using BOS.

In conclusion, the enhancements made to the BOS algorithm, through integrating advanced mathematical models such as Kalman filtering, stochastic processes, and wavelet transformations, can significantly expand its applicability across various domains. By continuing to refine these techniques and exploring further applications, such as in biological systems or high-speed fluid dynamics, the BOS method will undoubtedly serve as a critical asset in both research and industrial applications.

5. Conclusion

In this paper, we presented a robust, advanced BOS system that significantly enhances edge detection sensitivity, resolution, and noise reduction through the application of wavelet-based multi-scale analysis and Kalman filtering. The system demonstrates considerable improvements in detecting subtle flow-related edges, resolving fine flow structures, and suppressing noise, especially in mobile environments. Our detailed mathematical formulations and performance evaluations reveal realistic improvements across all key metrics, ensuring practical applicability in various real-world scenarios. These advancements position our system as a valuable tool for high-precision flow visualization in challenging settings.

References

[1]. Raffel M. Background-oriented schlieren (BOS) techniques. *Experiments in Fluids*. 2015;56(3). doi:https://doi.org/10.1007/s00348-015-1927-5

[2]. Settles GS. *Schlieren and Shadowgraph Techniques*. Springer Berlin Heidelberg; 2001. doi:https://doi.org/10.1007/978-3-642-56640-0

[3]. Raffel M, Willert C, Wereley S, Jürgen Kompenhans. *Particle Image Velocimetry*. Springer Nature; 2007. doi:https://doi.org/10.1007/978-3-540-72308-0

[4]. Richard H, Raffel M. Principle and applications of the background oriented schlieren (BOS) method. *Measurement Science and Technology*. 2001;12(9):1576-1585. doi:https://doi.org/10.1088/0957-0233/12/9/325

[5]. Wu H, Xu F, Duan Y, et al. Spatio-Temporal Fluid Dynamics Modeling via Physical-Awareness and Parameter Diffusion Guidance. arXiv.org. Published 2024. Accessed August 19, 2024. https://arxiv.org/abs/2403.13850

[6]. Doss N, Wu Y, Yang P, Zhou HH. Optimal estimation of high-dimensional location Gaussian mixtures. arXiv.org. Published 2020. Accessed August 19, 2024. https://arxiv.org/abs/2002.05818

[7]. Pedregosa F, Pedregosa@inria F, Fr, et al. Scikit-learn: Machine Learning in Python Gaël Varoquaux Bertrand Thirion Vincent Dubourg Alexandre Passos PEDREGOSA, VAROQUAUX, GRAMFORT ET AL. Matthieu Perrot Edouard Duchesnay. *Journal of Machine Learning Research*. 2011;12(12):2825-2830.

https://www.jmlr.org/papers/volume12/pedregosa11a/pedregosa11a.pdf

[8]. Xu K, Wen L, Li G, Bo L, Huang Q. Spatiotemporal CNN for Video Object Segmentation. *arXiv:190402363 [cs]*. Published online April 4, 2019. Accessed December 6, 2022. https://arxiv.org/abs/1904.02363

[9]. Oisin Mac Aodha, Humayun A, Pollefeys M, Brostow GJ. Learning a Confidence Measure for Optical Flow. *IEEE Transactions on Pattern Analysis and Machine Intelligence*. 2013;35(5):1107-1120. doi:https://doi.org/10.1109/tpami.2012.171

[10]. Mallat SG. A theory for multiresolution signal decomposition: the wavelet representation. *IEEE Transactions on Pattern Analysis and Machine Intelligence*. 1989;11(7):674-693. doi:https://doi.org/10.1109/34.192463

[11]. *Introduction to the Discrete Wavelet Transform (DWT)*.; 2004. https://mil.ufl.edu/nechyba/www/eel6562/course_materials/t5.wavelets/intro_dwt.pdf

[12]. Liu L, Su X, Wang G. On Inversion of Continuous Wavelet Transform. *Open Journal of Statistics*. 2015;05(07):714-720. doi:https://doi.org/10.4236/ojs.2015.57071

[13]. Unser M. Texture classification and segmentation using wavelet frames. *IEEE Transactions on Image Processing*. 1995;4(11):1549-1560. doi:https://doi.org/10.1109/83.469936

[14]. Szeliski R. *Computer Vision*. Springer London; 2011. doi:https://doi.org/10.1007/978-1-84882-935-0

[15]. Otsu N. A Threshold Selection Method from Gray-Level Histograms. *IEEE Transactions on Systems, Man, and Cybernetics*. 1979;9(1):62-66. doi:https://doi.org/10.1109/tsmc.1979.4310076

[16]. Scarano F, Riethmuller ML. Iterative multigrid approach in PIV image processing with discrete window offset. *Experiments in Fluids*. 1999;26(6):513-523. doi:https://doi.org/10.1007/s003480050318

[17]. Smith SM, Brady JM. SUSAN—A New Approach to Low Level Image Processing. *International Journal of Computer Vision*. 1997;23(1):45-78. doi:https://doi.org/10.1023/a:1007963824710

[18]. Schwab M, Mayr A, Haltmeier M. Deep Gaussian mixture model for unsupervised image segmentation. arXiv.org. Published 2024. https://arxiv.org/abs/2404.12252